

Synthesis and Properties of Metallo-Supramolecular Poly(*p*-xylylene)s

Daniel Knapton, Parameswar K. Iyer,[†] Stuart J. Rowan,* and Christoph Weder*

Department of Macromolecular Science and Engineering, Case Western Reserve University,
2100 Adelbert Road, Cleveland, Ohio 44106-7202

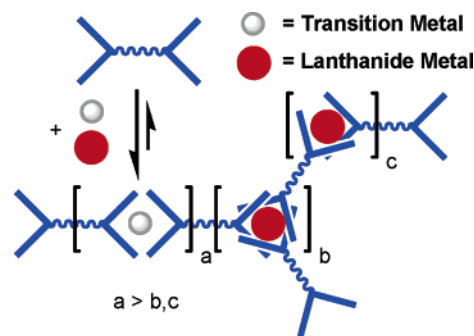
Received March 6, 2006; Revised Manuscript Received April 14, 2006

ABSTRACT: The self-assembly polymerization of ditopic macromolecules via metal–ligand binding offers a facile route to the preparation of metallo-supramolecular polymers. We herein report the utilization of this approach for the synthesis of arylene alkylene metallopolymers, which combine ease of processing with good high-temperature stability. The materials are based on a poly(2,5-dioctyloxy-*p*-xylylene) macromonomer that was prepared by in-situ end-capping of a low-molecular-weight poly(2,5-dioctyloxy-*p*-phenylene ethynylene) core with 2,6-bis(1'-methylbenzimidazolyl)-4-ethynylpyridine (Mebip) ligands and subsequent reduction under Hahn diimide conditions. The supramolecular polymerization of this macromonomer with equimolar amounts of Zn²⁺ or Fe²⁺ and a small amount of La³⁺, which can bind three Mebip ligands and causes cross-linking and/or branching, resulted in materials which offer excellent mechanical properties. The thermomechanical properties of the new polymers were investigated by a variety of techniques, including modulated differential scanning calorimetry, dynamic mechanical thermoanalysis, and thermogravimetric analysis.

Introduction

In our continuing efforts to develop high-temperature-stable organic/inorganic hybrid polymers, we embarked on the exploration of a new class of metallo-supramolecular polymers. The molecular design utilized in the present study merges the chemical structure of poly(arylene alkylene)s,¹ which offer outstanding thermal and mechanical properties, with the inherent processing advantages of dynamic (reversible) polymerization.² Poly(*p*-xylylene) (PPX)³ is the most prominent representative of the poly(arylene alkylene) family. This polymer and its derivatives are well-known for an appealing combination of high thermal stability excellent solvent resistance, high degree of crystallinity, low dielectric permittivity, and outstanding barrier properties.^{4,5} In addition, PPX exhibits excellent mechanical properties with a Young's modulus and a tensile strength of 2.4 GPa and ca. 47 MPa, respectively.⁴ Thus, PPX is an attractive material for many applications, including packaging of electronic components, medical device fabrication, and artifact conservation.⁴ Unfortunately, broad industrial exploitation of PPX is stifled by the obstacles which the material presents to conventional processing technologies.⁶ The high melting temperature of PPX (424 °C) is from an application point of view highly attractive, but it overlaps with the onset of thermal degradation, which prevents the melt-processing of PPX.⁷ In addition, PPX displays, even at elevated temperatures, a very low solubility in nearly all common solvents, thus thwarting solution-based processing options.⁶ As a result, the only practical approach for the synthesis and processing of PPX is by chemical vapor deposition⁸ (CVD) polymerization, which involves the vapor phase pyrolysis of [2.2]paracyclophanes,⁹ diesters of α,α' -dihydroxy-*p*-xylenes,¹⁰ or α -bromo-*p*-xylenes¹¹ and the subsequent polymerization of the resulting 1,4-quinodimethanes upon deposition on a cold substrate.¹² Several alternative approaches to prepare PPX derivatives or PPX-analogous polymers with an enhanced processability have been

Scheme 1. Schematic Representation of the Metallo-Supramolecular Polymerization of Ditopic Ligands with Both Transition and Lanthanide Metal Ions



proposed, involving the increase of the number of methylene groups comprised in the polymer backbone^{1,13} as well as the introduction of solubilizing side chains.^{11,14,15} Unfortunately, most of these polymers, when compared to the original PPX, exhibit a dramatically reduced crystallinity—some materials are fully amorphous—and show low melting or glass transition temperatures and thus have largely failed to substitute PPX in practical applications. We show here that this dilemma can, in part, be solved by utilizing a supramolecular polymerization process, as it allows for the assembly of high-molecular-weight polymeric aggregates from well-defined, easy-to-process precursors.² As several recent studies have demonstrated, a variety of noncovalent interactions can be utilized to assemble a wealth of different monomers.^{2b,c} One particularly useful and well-studied means of preparing supramolecular polymers is the utilization of metal–ligand interactions (Scheme 1).^{16–20} A wide variety of metal–ligand binding motifs are available that offer a broad range of binding characteristics (e.g., thermodynamic and kinetic stabilities),²¹ which in turn can be utilized to tune the nature of the resulting supramolecular materials.²² Building on our previous work on the metal–ligand based self-assembly of poly(2,5-dialkyloxy-*p*-phenylene ethynylene)s²³ (PPEs) and exploiting a reaction methodology developed in our laboratories for the reduction of PPEs to their corresponding PPX derivatives,¹⁵ we herein report the utilization of this approach for the

[†] Present address: Department of Chemistry, Indian Institute of Technology, North Guwahati-781039, Assam, India.

* Corresponding authors. E-mail: stuart.rowan@case.edu, christoph.weder@case.edu.

synthesis of arylene alkylene metallopolymers, which combine ease of processing with good mechanical characteristics and high-temperature stability. We have chosen the following building blocks for the supramolecular polymers investigated here: (i) a low-molecular-weight poly(2,5-dioctyloxy-*p*-xylylene), as a PPX segment¹⁵ whose thermal properties have been previously investigated; (ii) a model compound mimicking a single *p*-xylylene unit; (iii) the 2,6-bis(1'-methylbenzimidazolyl)-pyridine (Mebip) ligand as the binding unit,²⁴ which is thermally stable and useful as a metal ion binding motif in supramolecular polymerizations;²⁵ (iv) a mixture of Fe(ClO₄)₂ and La(ClO₄)₃, which cause linear chain extension (Fe²⁺) and branching/cross-linking (La³⁺), respectively (Scheme 1).

Experimental Section

General Methods. NMR spectra were recorded on a Varian 600 MHz NMR spectrometer. Gel permeation chromatography (GPC) data were calibrated against polystyrene standards and collected on a Varian Prostar equipped with a model 350 RI detector and a PSS SDV linear M column with THF as an eluent. Dynamic mechanical thermoanalysis (DMTA) measurements were made on a Perkin-Elmer dynamic mechanical analyzer 7e performing single frequency/constant stress (1 Hz, 40 kPa dynamic, and 44 kPa static) experiments on rectangular films at a heating rate of 3 °C/min. Thermogravimetric analysis (TGA) was carried out on a TA Instruments TGAQ500 under N₂ at a heating rate of 10 °C/min. Modulated differential scanning calorimetry (MDSC) was carried out on a TA Instruments DSCQ200 under N₂ at a heating rate of 2 °C/min. Ultraviolet–visible (UV–vis) absorption spectra were obtained on a Perkin-Elmer Lambda 800 spectrometer. Steady-state photoluminescence (PL) spectra were acquired on a PTI C720 fluorescence spectrometer. Spectra were collected under excitation at 320 and 400 nm and are corrected for the instrument throughput and the detector response. MALDI time-of-flight (TOF) mass spectroscopy was carried out on a Bruker BIFLEX III mass spectrometer. Wide-angle X-ray diffraction (WAXD) measurements were conducted using a Rigaku SA-HF3 X-ray generator in combination with a D/MAX2000/PC series diffractometer. For the WAXD experiments, film samples were placed on a glass cover slide aligned in the path of the wide-angle diffractometer.

Materials. Ethynyls **1a**^{23a} and **1b**^{23b} were prepared according to literature procedures. Unless otherwise stated, all other reagents, solvents, metal complexes, and catalysts were purchased from Aldrich Chemical Co., Fisher Scientific, or Strem Chemicals and were used without further purification. Distilled spectroscopic grade CHCl₃ (passed through a plug of basic alumina) and spectroscopic grade CH₃CN (Aldrich) were employed for the optical absorption and emission experiments as well as for the metallopolymerization reactions. Toluene, xylenes, and tripropylamine were distilled from CaH₂ under an inert atmosphere.

Synthesis of Xylylene 2a. Ethynylene **1a** (173 mg, 0.164 mmol), *p*-toluenesulfonyl hydrazide (TSH) (305.4 mg, 1.64 mmol), and tripropylamine (TPA) (0.31 mL, 1.64 mmol) were dissolved in toluene (8.7 mL), and the solution was heated under reflux at 112 °C. After 3 h, an additional portion of TSH (153 mg, 0.82 mmol) was added, and the reaction mixture was heated under reflux for another 2 h. The hot reaction mixture was passed through basic alumina, and the plug was subsequently washed with a minimal amount of hot toluene. The combined organic fractions were washed twice with deionized water and dried over Na₂SO₄, and the solvents were evaporated in vacuo. The resulting solid was redissolved in a minimal amount of CHCl₃, and the product was precipitated from cold, rapidly stirred MeOH. The resulting solid was collected and recrystallized twice first from benzene and then from toluene, yielding **2a** as an off-white solid (35 mg, 20%). ¹H NMR (600 MHz, CDCl₃): δ 8.32 (s, 4 H), 7.88 (d, 4 H, *J*_{H–H} = 7.8 Hz), 7.47 (d, 4 H, *J*_{H–H} = 7.8 Hz), 7.37 (m, 8 H), 6.73 (s, 2 H), 4.25 (s, 12 H), 3.94 (t, 4 H, 6.6 Hz), 3.07 (m, 4 H), 3.04 (m, 4 H), 1.80 (m, 4 H), 1.45 (m, 4 H), 1.32 (m, 4 H), 1.24 (m, 4 H), 1.19 (m, 8 H),

0.80 (t, 6 H, *J*_{H–H} = 6.8 Hz). ¹³C NMR (CDCl₃, 125 MHz): δ 153.9, 150.4, 142.5, 137.0, 127.8, 125.4, 123.5, 122.7, 120.1, 113.9, 109.8, 68.8, 36.2, 31.9, 31.8, 29.6, 29.4, 29.3, 26.3, 22.7, 14.2. MALDI–TOF MS *m/z* 1066.0 (M⁺, C₆₈H₇₆N₁₀O₂ requires 1065.4).

Synthesis of Xylylene 2b. Ethynylene **2a** (200 mg, 0.561 mmol), TSH (1.05 g, 5.62 mmol), and TPA (1.07 mL, 5.62 mmol) were dissolved in xylenes (23 mL), and the solution was heated under reflux at 140 °C. After 2 h, an additional portion of TSH (1.05 g, 5.62 mmol) and TPA (1.07 mL, 5.62 mmol) was added, and the reaction mixture was heated under reflux for another 3 h. The hot reaction mixture was passed through basic alumina, and the plug was subsequently washed with a minimal amount of hot toluene. The combined organic fractions were washed twice with deionized water and added dropwise to a rapidly stirred solution of MeOH. After stirring for 2 h, the off-yellow precipitate was collected and washed with boiling MeOH, EtOH, CH₃CN, and room temperature MeOH. Drying overnight under vacuum at 40 °C yielded **2b** as a pale yellow solid (137 mg, 70%). ¹H NMR (600 MHz, CDCl₃): δ 8.34 (s, 4 H, end group), 7.88 (d, 2 H, *J*_{H–H} = 7.8 Hz, end group), 7.47 (d, 2 H, *J*_{H–H} = 7.8 Hz, end group), 7.37 (m, 8 H, end group), 6.72 (s, 2 H, Ar end group), 6.07 (s, 2 H, Ar), 4.25 (s, 12 H, end group), 3.91 (t, 2 H, *J*_{H–H} = 6 Hz, OCH₂ end group), 3.89 (t, 4 H, *J*_{H–H} = 6 Hz, OCH₂), 3.09 (m, 4 H, Ar–CH₂–CH₂–Ar end group), 3.04 (m, 4 H, Ar–CH₂–CH₂–Ar end group), 2.83 (bs, 4 H, Ar–CH₂–CH₂–Ar), 2.32 (s, toluene impurity), 1.81 (m, 4 H), 1.49 (m, 4 H), 1.34 (m, 4 H), 1.27 (m, 12 H), 0.87 (t, 6 H, *J*_{H–H} = 6.6 Hz), 0.79 (t, 6 H, *J*_{H–H} = 6.6 Hz, CH₃ end group). *X*_n = 25 (*M*_n = 9700) by ¹H NMR. ¹³C NMR (CDCl₃, 125 MHz): δ 150.7, 149.5, 142.6, 137.2, 129.3, 125.5, 123.5, 122.8, 120.2, 114.2, 109.8, 68.9, 36.3, 31.9, 31.3, 29.8, 29.7, 29.5, 29.4, 26.3, 22.7, 14.1. GPC (THF): PDI = 1.4; *M*_n = 10 067; *M*_w = 14 094.

Typical Sample Preparation of Metallo-Supramolecular Polymer. To a stirred solution of xylylene **2b** (71.4 mg, 7.35 μmol) in 0.5 mL of CHCl₃ (14.7 mM) was first added a solution of La-(ClO₄)₃ in CH₃CN (81 μL of a 0.0081 M solution) followed by a solution of Fe(ClO₄)₂ in CH₃CN (32.5 μL of a 0.206 M solution). Immediately upon the addition of Fe²⁺, the mixture became purple and highly viscous. Further dilution with CHCl₃ (4 mL) allowed the mixture to be transferred as a liquid to a cylindrical aluminum film caster (diameter 3 cm) with Teflon base. The solvent was slowly evaporated at room temperature over the course of 18 h. The resulting purple film (diameter: 28 mm; thickness: ~140 μm) was removed from the mold, dried under vacuum for 48 h at room temperature and 24 h at 30 °C, and cut into smaller pieces for various analyses.

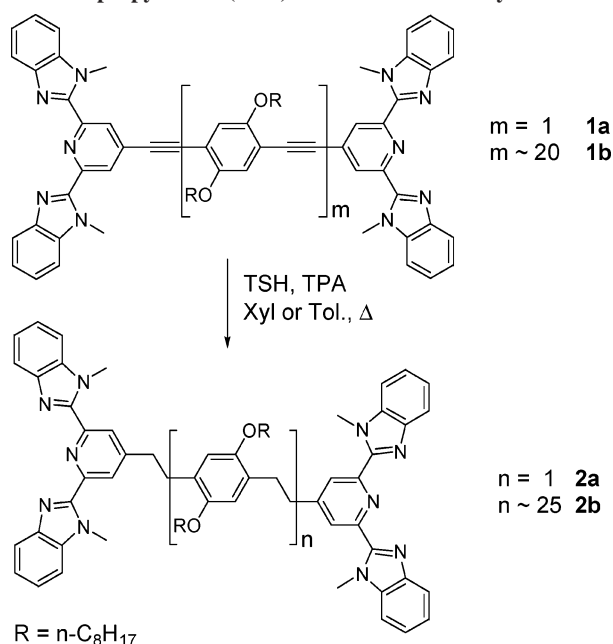
General Procedure for UV–vis Titrations with Zn(ClO₄)₂. A solution of **2b** (0.022 mM) in a mixture of CHCl₃/CH₃CN (9/1 v/v) was titrated with 30 μL aliquots of a solution of Zn(ClO₄)₂ (0.17 mM) and **2b** (0.022 mM) in the same solvent mixture. The addition was done stepwise, and after each step, the formation of [2b·Zn(ClO₄)₂]_n was monitored by UV–vis spectroscopy. After a ratio 1:1 of **2b**:Zn²⁺ was reached, the mixture was equilibrated for 30 min in each titration step before UV–vis analysis and the next subsequent addition of Zn(ClO₄)₂ and **2b**.

Results and Discussion

Synthesis of Ditopic Monomers 2a and 2b. Expanding on our previous work on the metal–ligand-based self-assembly of Mebip-end-capped poly(2,5-dialkyloxy-*p*-phenylene ethynylene)s,²³ we targeted here the synthesis of the ditopic Mebip-end-capped PPX macromonomer **2b** and the corresponding monodisperse low-molecular-weight ditopic model monomer **2a** (Scheme 2).

Following a reaction methodology developed previously,¹⁵ the Mebip end-capped xylylene species **2a** and **2b** were prepared from their corresponding and previously described²³ ethynylene precursors **1a** and **1b** via diimide reduction chemistry utilizing *p*-toluenesulfonylhydrazide (TSH) and tripropylamine (TPA) in hot toluene or xylenes (Scheme 2).²⁶ Compound **2a** was

Scheme 2. Synthesis of Mebip-End-Capped Xylylenes **2a** and **2b** via Hydrogenation of Mebip-End-Capped Aryl Ethynyls **1a** and **1b** with *p*-Toluenesulfonyl Hydrazide (TSH) and Tripropylamine (TPA) in Hot Toluene or Xylenes



extensively purified via precipitation from MeOH followed by recrystallization from both hot benzene and toluene. Characterization by ^1H NMR, ^{13}C NMR, and MALDI-TOF MS confirmed the chemical structure as well as high structural purity of the material at hand. Compound **2b** was isolated by precipitation from MeOH followed by extensive washing with a battery of solvents, as described in detail in the Experimental Section. The nature of the side chains (*n*-octyloxy) and the number-average degree of polymerization, X_n , of ~ 20 (determined by ^1H NMR end-group analysis) of the starting compound **1b** were chosen to provide for adequate solubility.¹⁵ Indeed, xylylene **2b** was completely soluble in CHCl_3 at concentrations of up to at least ~ 140 mg/mL. The macromonomer **2b** was characterized to satisfaction by ^1H and ^{13}C NMR spectroscopy. Other than the appearance of a prominent resonance around 2.83 ppm, corresponding to the new $\text{Ar}-\text{CH}_2-\text{CH}_2-\text{Ar}$ moieties, two weaker signals at 3.09 and 3.04 ppm are observed in the ^1H NMR spectrum which, on the basis of previous HMQC studies on a phenyl-end-capped analogue,¹⁵ we assign to the methylene units connected to the Mebip end groups. The signal of the aromatic protons experiences a shift to lower field upon reaction, reflecting the reduction of the electron-withdrawing ethynylene units. The similarity of the integrals of the diagnostic methylene units (OCH_2 and $\text{Ar}-\text{CH}_2-\text{CH}_2-\text{Ar}$) and the absence of the aromatic signal characteristic of the starting material indicates complete conversion to **2b** (see Supporting Information for spectra). ^1H NMR end-group analysis, which involved both Mebip and various polymer backbone and side chain signals, evidenced that the reduction caused a slight increase of X_n to ca. 25. This finding is consistent with the loss of low-molecular-weight material during workup and indicates that little or no chain cleavage occurred during the reduction. Gel permeation chromatography (GPC) data reveal an X_n of ~ 28 with a PDI of 1.4 and nicely confirm the NMR end-group analysis data (see Supporting Information for GPC traces). The absence of end-group signals other than the ones expected for the Mebip groups and the good agreement of the values of X_n determined by NMR and GPC point to the fact that xylylene **2b** is at least to a high degree end-capped with Mebip groups.

Table 1. Optical Absorption and PL Emission Data of Solutions of Ethynyls **1a** and **1b**, Xylylenes **2a** and **2b**, and the Supramolecular Polymer $[\mathbf{2b} \cdot \text{Fe}(\text{ClO}_4)_2/\text{La}(\text{ClO}_4)_3]_n$

compound ^a	absorption λ_{max} (nm)	emission λ_{max} (nm)
1a	321, 352, 390	448 ^b
2a	318	369, 480 ^b
1b	319, 448	484, 510 ^c
2b	300, 330	367, 485 ^b
$[\mathbf{2b} \cdot \text{Fe}(\text{ClO}_4)_2/\text{La}(\text{ClO}_4)_3]_n$	n.a.	— ^d

^a All measurements were carried out in 9:1 (v/v) $\text{CHCl}_3/\text{CH}_3\text{CN}$ solutions, except for $[\mathbf{2b} \cdot \text{Fe}(\text{ClO}_4)_2/\text{La}(\text{ClO}_4)_3]_n$, which was measured at a concentration of 6.6 mg/mL in CHCl_3 . ^b Excitation at 320 nm. ^c Excitation at 400 nm. ^d Emission is fully quenched; see Supporting Information.

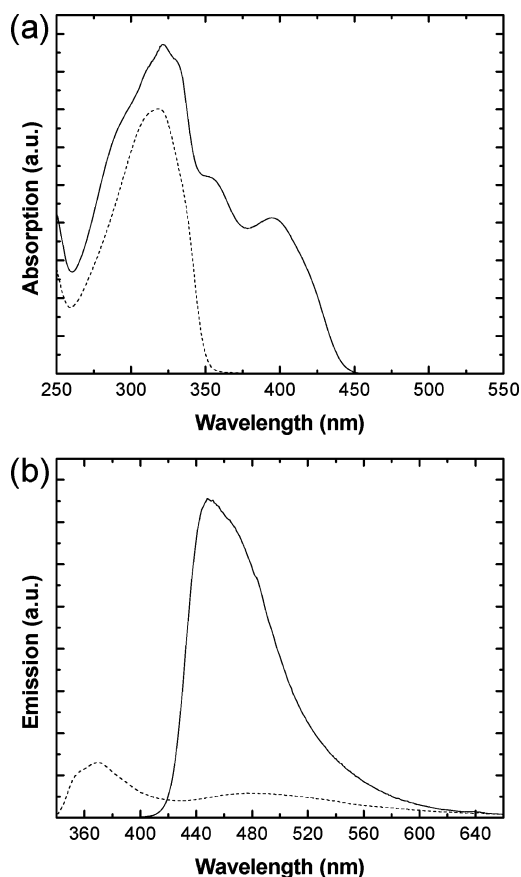


Figure 1. Optical absorption (a) and PL emission spectra (b) of ethynylene **1a** (solid) and xylylene **2a** (dashed) in 9:1 (v/v) $\text{CHCl}_3/\text{CH}_3\text{CN}$. Emission spectra were collected with excitation at 320 nm.

It should be noted that this factor is of high importance to the effective self-assembly of this macromonomer.

Optical Properties of Ditung Monomers **2a and **2b**.** Optical spectroscopy is an outstanding tool to probe the various species created upon metal-induced polymerization and allows for a unique elucidation of the self-assembly process (vide infra). We therefore investigated the photophysical characteristics of ditopic monomers **2a** and **2b** in detail. All spectroscopic data were obtained in $\text{CHCl}_3/\text{CH}_3\text{CN}$ solution and are summarized in Table 1; absorption and photoluminescence (PL) emission spectra are shown in Figures 1 and 2. The data of the conjugated precursors **1a** and **1b**²³ are included for reference purposes.

Not surprisingly, the characteristic absorption bands related to the $\pi-\pi^*$ transitions of the conjugated ethynylene backbones (390 and 448 nm) completely disappeared upon reduction, and **2a** and **2b** are essentially transparent at wavelengths above 350 nm (Figures 1 and 2). Model compound **2a** displays an absorption band with maximum, λ_{max} , at 318 nm, which can be

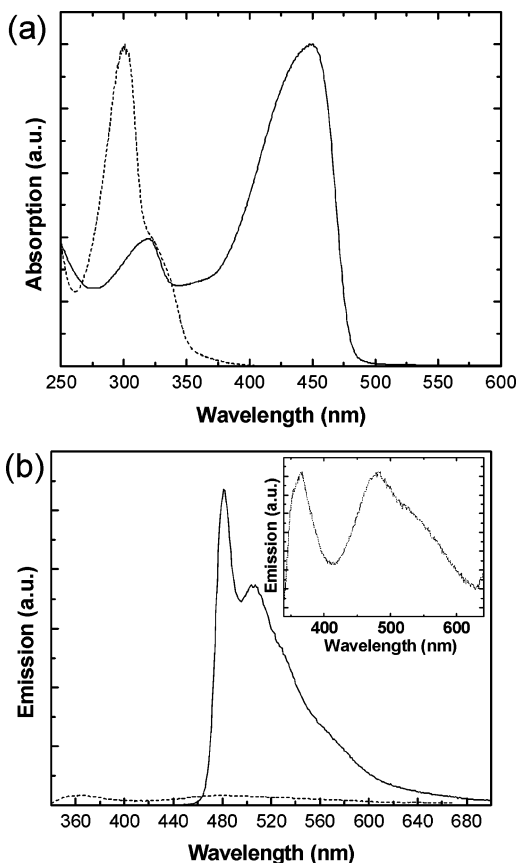


Figure 2. Optical absorption (a) and PL emission spectra (b) of ethynylene **1b** (solid) and xylene **2b** (dashed) in 9:1 (v/v) CHCl_3 : CH_3CN . Inset in (b): Magnification (30 \times) of the emission spectrum of **2b**.

attributed to the π - π^* transition related to the Mebip moiety.^{23,25c} Macromonomer **2b** displays a narrow absorption band centered around 300 nm and a shoulder at ca. 330 nm; we interpret the main band with the π - π^* transition of the 2,5-dialkoxy-*p*-xylylene moieties²⁷ and confirmed via an excitation PL scan (see Supporting Information) that the shoulder is indeed related to the π - π^* transition of the Mebip ligand. Optical excitation of the ethynylene precursors **1a** and **2a** causes intense photoluminescence. The corresponding steady-state emission spectra (Figures 1 and 2) display well-resolved bands that exhibit features consistent with π - π^* fluorescence of the conjugated phenylene ethynylene segments.^{23,28} As expected, the emission associated with these moieties is virtually fully suppressed upon hydrogenation. In both xylenes, **2a** and **2b**, a weak emission band with a λ_{max} of ~ 367 – 369 nm can be observed, which is characteristic of the π - π^* transition related to the Mebip moiety.²⁵ The PL emission spectra of both reduced species, **2a** and **2b**, show an additional weak emission band centered at ~ 480 and 485 nm, respectively, similar to poly(2,5-dialkoxy-*p*-xylylene)s without Mebip end groups that were prepared before by the same reduction method.¹⁵ Excitation spectra (see Supporting Information) indicate that the emission is not an intrinsic feature of either the 2,5-dialkoxy-*p*-xylylene or Mebip motif. The fact that a similar emission band is observed for the different materials investigated and the fact that the emission persists in dilute solutions also seems to exclude the formation of excimers. This emission may be indicative of incomplete reduction or the presence of impurities, but neither ^1H NMR nor MALDI-TOF MS (compound **2a**) shows any evidence for such defects or impurities, strongly suggesting that such contaminants are present at an acceptable subpercent level.

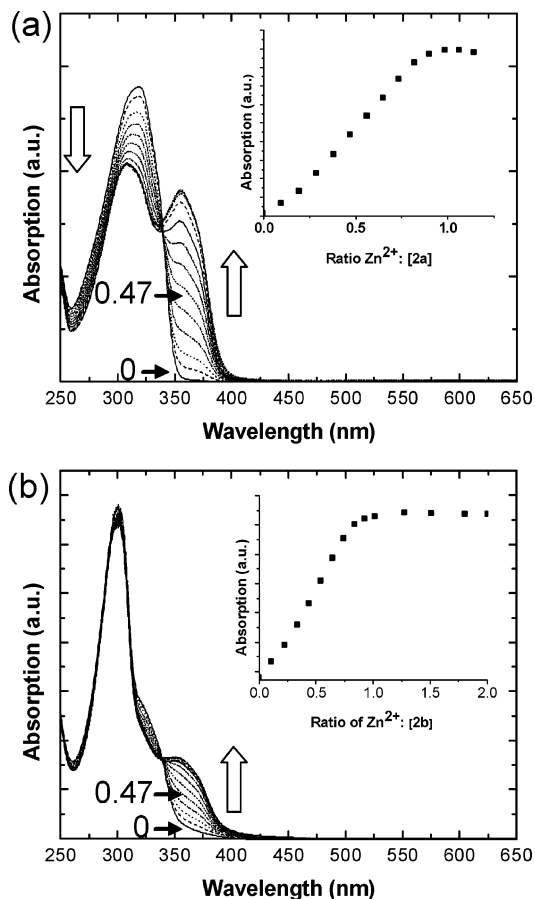


Figure 3. UV-vis spectra acquired upon titration of **2a** (0.025 mM) (a) and **2b** (0.022 mM) (b) in 9:1 (v/v) CHCl_3 : CH_3CN with $\text{Zn}(\text{ClO}_4)_2$. Shown are spectra of Zn^{2+} :**2a** ratios between 0 and 1.14 and Zn^{2+} :**2b** ratios between 0 and 2.01. The insets show the normalized absorption at 360 and 370 nm as a function of Zn^{2+} :**2a** and Zn^{2+} :**2b** ratios, respectively.

Self-Assembly and Solution Properties of the Metallo-Supramolecular Polymers of **2a and **2b**.** The formation of metallo-supramolecular species, $[\mathbf{2a} \cdot \text{MX}_n]_n$ and $[\mathbf{2b} \cdot \text{MX}_n]_n$, is readily achieved by the addition of 1 equiv of an appropriate metal ion salt to a solution of the Mebip end-capped xylenes **2a** and **2b**. We found that a variety of metal ions display appropriate interactions (i.e., large equilibrium constants and rapid complexation kinetics) that allow for supramolecular polymerization using the terdentate Mebip motif.²⁵ Encouraged by the successful metallopolymerization of Mebip-end-capped PPEs with Zn^{2+} and Fe^{2+} ,^{23b} we opted to employ these metal ions in the present study. To probe the complexation characteristics of **2a** and **2b**, we first conducted a detailed optical titration study with Zn^{2+} , which offers both a large equilibrium constant and rapid complexation kinetics. To this end, $\text{Zn}(\text{ClO}_4)_2$ was titrated into solutions of **2a** and **2b**, and the resulting products were analyzed by means of UV-vis spectroscopy (Figure 3). It should be noted that precipitation, presumably of high-molecular-weight macromolecules, was observed when these experiments were carried out at too high concentrations; this dictated that the UV-vis titrations be performed at a concentration of 22–25 μM of the respective ditopic ligands. As such, these conditions clearly favor the formation of oligomeric species as opposed to high-molecular-weight aggregates. The addition of Zn^{2+} to xylenes **2a** and **2b** rendered the originally colorless solutions pale yellow. In both cases a new lowest-energy absorption band was observed, centered at 354 nm in the case of **2a** and 360 nm in the case of **2b** (Figure

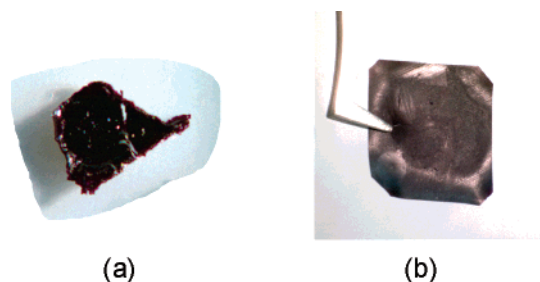


Figure 4. (a) Pictures of solution-cast films (CHCl_3) of the metallo-supramolecular polymers $[\mathbf{2b} \cdot \text{Fe}(\text{ClO}_4)_2]_n$ (a) and $[\mathbf{2b} \cdot \text{Fe}(\text{ClO}_4)_2]/\text{La}(\text{ClO}_4)_3]_n$ (b).

3). Concomitantly, in model compound **2a** the intensity of the initial absorption band with λ_{max} at 318 nm associated with the $\pi-\pi^*$ transition related to the Mebip moiety was significantly reduced upon binding, as was the related absorption of macromonomer **2b** observed as a shoulder at ~ 330 nm. The spectra of both titration series exhibit a single isosbestic point at ~ 340 nm up to a $\text{Zn}^{2+}:\mathbf{2}$ ratio of approximately one, suggesting equilibria between the bound and unbound monomers **2a** and **2b**. At $\text{Zn}^{2+}:\mathbf{2}$ ratios greater than one, new isosbestic points are observed, which appear to correspond to the presence of chain-terminating monomer– Zn^{2+} –solvent complexes formed upon depolymerization of the supramolecular species in the presence of an excess of metal.^{23a} We further quantified the spectral changes observed in the above-discussed Zn^{2+} titrations as the normalized intensity of the emerging absorption bands; the data are plotted in the insets of Figure 3. Gratifyingly, the changes are virtually identical for the well-defined monodisperse model compound **2a** and the macromonomer **2b**, leveling off at a $\text{Zn}^{2+}:\mathbf{2}$ ratio of 1:1, which is consistent with the ditopic nature of the monomers and the successful self-assembly in dilute solution. Similar titration data were obtained upon addition of $\text{Fe}(\text{ClO}_4)_2$ to **2b** (for this experiment a different batch of **2b** of slightly higher X_n (32) was utilized; see Supporting Information for spectra). In this case, a characteristic^{23b,25c,29} metal-to-ligand charge-transfer absorption band was observed at 570 nm.

Preparation and Solid-State Optical Properties of Metallo-Supramolecular Polymers Based on **2b.** Monomer **2b** is a pale yellow powder, which is soluble in chloroform and can readily be spin- or solution-cast into homogeneous thin films. However, these films do not display self-supporting mechanical properties. The preparation and processing of metallo-supramolecular polymers based on **2b** and $\text{Zn}(\text{ClO}_4)_2$ or $\text{Fe}(\text{ClO}_4)_2$ ($[\mathbf{2b} \cdot \text{M}]_n$) followed the protocol developed for similar materials comprising a Mebip-end-capped poly(2,5-dialkyloxy-*p*-phenylene ethynylene) **1b** of an X_n similar to that of **2b**,²³ which display outstanding mechanical properties. The procedure involved codissolution of **2b** and an equimolar amount of either of the metal salts in a $\text{CHCl}_3/\text{CH}_3\text{CN}$ mixture, followed by solution casting. The addition of either $\text{Zn}(\text{ClO}_4)_2$ or $\text{Fe}(\text{ClO}_4)_2$ in CH_3CN to **2b** in CHCl_3 resulted in solutions of $[\mathbf{2b} \cdot \text{Zn}(\text{ClO}_4)_2]_n$ and $[\mathbf{2b} \cdot \text{Fe}(\text{ClO}_4)_2]_n$ which upon casting and drying yielded films that displayed poor mechanical properties (Figure 4a). To probe whether an increase of the X_n of the macromonomer would change this situation, the experiment was repeated with a macromonomer **2b** of an X_n of ~ 32 (see Supporting Information for synthesis of this macromonomer), but the behavior of this ditopic ligand was virtually the same. Thus, the $[\mathbf{2b} \cdot \text{M}]_n$ samples investigated here display mechanical properties that are clearly inferior when compared with the corresponding $[\mathbf{1b} \cdot \text{M}]_n$ analogues reported earlier.^{23b} The structural purity of **2b** established by NMR, the successful self-assembly in dilute solution established by optical titration, and the fact that the

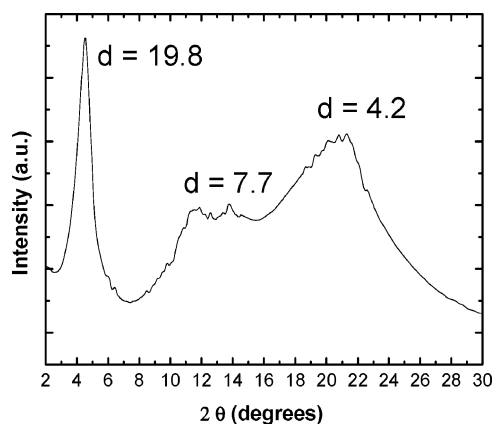


Figure 5. Wide-angle X-ray diffraction (WAXD) pattern of a solution-cast metallo-supramolecular polymer film of $[\mathbf{2b} \cdot \text{Fe}(\text{ClO}_4)_2]/\text{La}(\text{ClO}_4)_3]_n$.

binding strength of **2b** should be similar to that of **1b** and many related systems²⁵ suggests that the $[\mathbf{2b} \cdot \text{M}]_n$ supramolecular materials prepared here are indeed of polymeric nature. Thus, the observation of poor mechanical properties seems to reflect the lack or low concentration of chain entanglements and indicates weak intermolecular interactions between the individual supramolecular chains.

With the objective to improve the material's mechanical properties, we employed minor amounts of lanthanide perchlorate salts, which are well-known to bind three Mebip ligands,³⁰ as a cross-linking/branching unit in our supramolecular polymerization of **2b** and $\text{Fe}(\text{ClO}_4)_2$ (Scheme 1). To generate the cross-links/branch points in a metal ion:**2b** system that was processed as described above, 9 mol % $\text{La}(\text{ClO}_4)_3$ (with respect to **2b**) in CH_3CN was added to xylylene **2b** in CHCl_3 (71.4 mg/mL) with the assumption of a 3:1 Mebip: La^{3+} binding motif. The further addition of 91 mol % $\text{Fe}(\text{ClO}_4)_2$ in CH_3CN resulted in an instantaneous and dramatic visual increase of the solution's viscosity, illustrating the successful linear chain growth (via 2:1 Mebip:**2b** binding) of the preformed 3:1 Mebip: La^{3+} complexes. Solution casting and slow evaporation of the solvent led to purple films, which displayed appreciable mechanical properties (Figure 4b). The deep purple color of the material results virtually exclusively from a metal-to-ligand charge transfer (MLCT), indicative of the formation of 2:1 Mebip: Fe^{2+} complexes, as the addition of $\text{La}(\text{ClO}_4)_3$ to **2b** resulted in the formation of only near colorless solutions.^{23b,25c,29} In addition, the PL emission associated with **2b** is fully quenched (Figure 2, Supporting Information). Figure 4b shows unequivocally that solution-processed objects from $[\mathbf{2b} \cdot \text{Fe}(\text{ClO}_4)_2]/\text{La}(\text{ClO}_4)_3]_n$ —very much in contrast to the neat xylylene **2b** and poly(2,5-dioctyloxy-*p*-xylylene)s¹⁵ of similar X_n but without Mebip end groups—exhibit appreciable mechanical strength and flexibility.

The solid-state structure of $[\mathbf{2b} \cdot \text{Fe}(\text{ClO}_4)_2]/\text{La}(\text{ClO}_4)_3]_n$ was investigated by wide-angle X-ray diffraction (WAXD). Three distinct peaks are discernible in the diffraction pattern (Figure 5). The most prominent and sharpest of the reflections occurs at $2\theta = 4.6^\circ$, corresponding to a d spacing of 19.8 Å. At higher 2θ values, two broad reflections are observed with d spacings of approximately 7.7 and 4.2 Å. Considering the stark similarity of these reflections to that of 2,5-dialkyloxy(*p*-phenyleneethynylene)s,²⁸ the WAXD data suggest that the morphology of the self-assembled system is lamellar and is largely driven by side-chain packing.

Thermomechanical Properties of $[\mathbf{2b} \cdot \text{Fe}(\text{ClO}_4)_2]/\text{La}(\text{ClO}_4)_3]_n$. The mechanical and thermal properties of $[\mathbf{2b} \cdot \text{Fe}(\text{ClO}_4)_2]/\text{La}(\text{ClO}_4)_3]_n$ films were investigated in more detail by means of

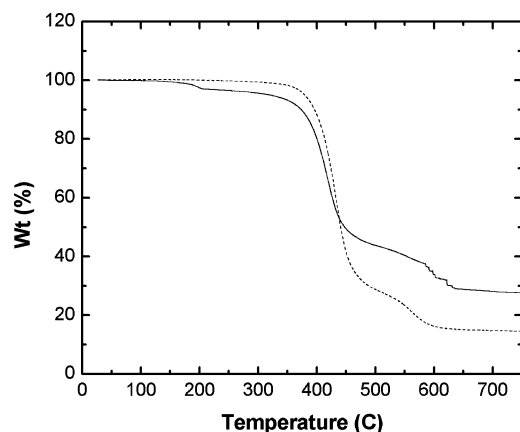


Figure 6. Thermogravimetric analysis (TGA) traces for $[2b \cdot Fe(ClO_4)_2/La(ClO_4)_3]_n$ (solid) and xylylene **2b** (dashed) under N_2 . The experiments were conducted at a heating rate of $10\text{ }^\circ\text{C/min}$.

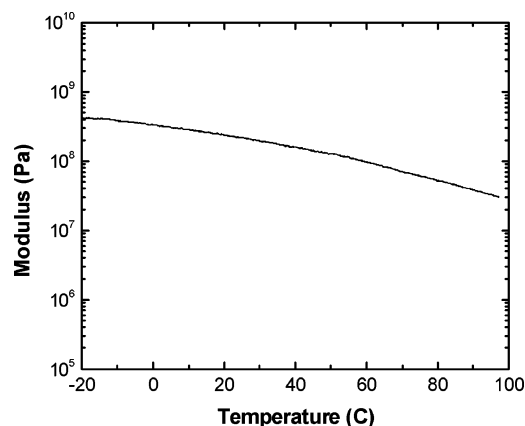


Figure 7. Dynamic mechanical thermoanalysis (DMTA) trace for $[2b \cdot Fe(ClO_4)_2/La(ClO_4)_3]_n$. The experiment was conducted under N_2 at a heating rate of $3\text{ }^\circ\text{C/min}$ and a frequency of 1 Hz.

thermogravimetric analysis (TGA), dynamic mechanical thermoanalysis (DMTA), and modulated differential scanning calorimetry (MDSC); these experiments were all conducted under a nitrogen atmosphere. TGA traces (Figure 6) of neat **2b** reveal an onset of significant weight loss (2%) at $354\text{ }^\circ\text{C}$, which has previously been related to the degradation of alkyl side chains.³¹ The supramolecular polymer $[2b \cdot Fe(ClO_4)_2/La(ClO_4)_3]_n$ shows a rather similar overall thermal behavior (Figure 6). For the materials investigated here, however, the initial 2% weight loss was observed at a substantially lower temperature ($193\text{ }^\circ\text{C}$), which we ascribe to the thermal degradation of the perchlorate counterions upon melting (vide infra) and are considering investigating in more detail.

The mechanical properties of $[2b \cdot Fe(ClO_4)_2/La(ClO_4)_3]_n$ were elucidated by DMTA in a temperature range of -20 to $100\text{ }^\circ\text{C}$ (Figure 7). The room temperature modulus was determined to be 220 MPa, placing the self-assembled system in the same regime as low-density polyethylene. The modulus decreased continuously as the temperature was increased, which may be on account of progressive decomplexation of the more weakly bound lanthanide–Mebip cross-links. To determine the melting temperature, T_m , of both **2b** and $[2b \cdot Fe(ClO_4)_2/La(ClO_4)_3]_n$, MDSC experiments were performed (Figure 8). The MDSC trace of neat **2b** clearly shows a reversible endotherm with maximum at $166\text{ }^\circ\text{C}$ corresponding to the T_m , which is virtually identical to that reported for a poly(2,5-diethoxy-*p*-xylylene) of similar X_n but without Mebip end groups ($170\text{ }^\circ\text{C}$).¹⁵ The MDSC trace of $[2b \cdot Fe(ClO_4)_2/La(ClO_4)_3]_n$ shows a largely irreversible exotherm at $176\text{ }^\circ\text{C}$ that we associate, by comparison

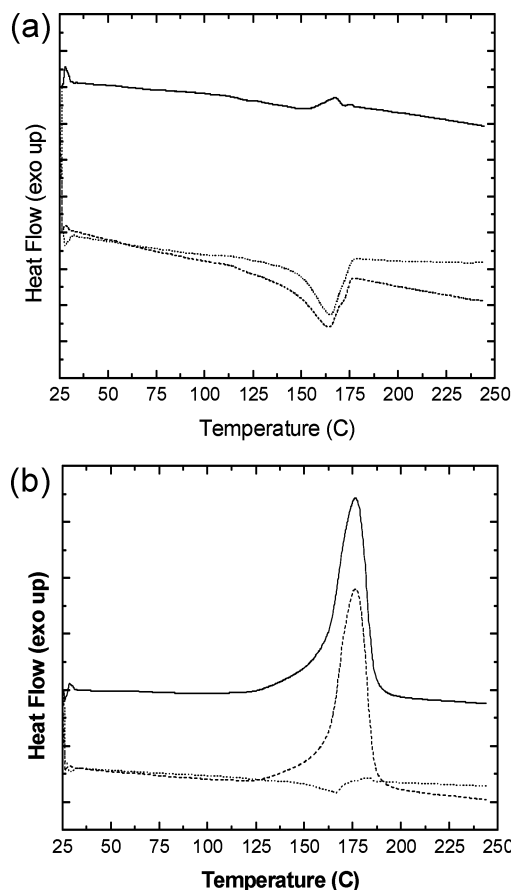


Figure 8. Modulated differential scanning calorimetry (MDSC) heating scans of **2b** (a) and $[2b \cdot Fe(ClO_4)_2/La(ClO_4)_3]_n$ (b) with nonreversible heat flow (solid), heat flow (dashed), and reversible heat flow (dotted). The experiments were conducted under N_2 at a heating rate of $2\text{ }^\circ\text{C/min}$.

with TGA data, to the degradation of the perchlorate counterions. The reversible portion of the scan shows a weak endotherm at $166\text{ }^\circ\text{C}$, which corresponds to melting at a temperature which is nearly identical to that of **2b**. Thus, the MDSC data suggest that the melt transition of the new metallo-supramolecular PPX is largely governed by the hydrocarbon building block and can be tailored to meet specific thermal demands by judicious design of the latter.

Conclusions

To develop thermally stable and easily processable poly(*p*-xylylene) derivatives, we utilized metal-ion-mediated self-assembly polymerization. We have demonstrated that the supramolecular metallopolymerization of PPX-type Mebip end-capped macromolecules with a mixture of Fe^{2+} and La^{3+} can be employed to produce materials that combine good mechanical characteristics with a solution-processing capability that cannot be attained with traditional PPX and its related derivatives.⁶ The introduction of La^{3+} as a metal which can bind three Mebip ligands and act as a cross-linking/branching unit was shown to be a most valuable design tool and in the case of the materials investigated here was key to achieving good mechanical characteristics. It appears that the use of dynamic polymerization offers a broadly useful means to attain thermally robust inorganic/organic hybrid materials without altering the properties associated with the macromolecular core and should be easily extendable to other thermally stable cores.

Acknowledgment. This material is based upon work supported by the U.S. Army Research Office (DAAD19-03-1-

0208). We acknowledge fruitful discussions with Drs. J. Benjamin Beck and Akshay Kokil.

Supporting Information Available: Experimental details for the synthesis of Mebip-end-capped poly(2,5-dioctyloxy-*p*-xylylene) with $X_n \sim 32$; GPC traces of **1b** and **2b**; PL emission spectra of **2b** and $[\mathbf{2b} \cdot \text{Fe}(\text{ClO}_4)_2/\text{La}(\text{ClO}_4)_3]_n$ and PL excitation spectra of **2b**; UV-vis absorption spectra acquired upon the titration of Mebip-end-capped poly(2,5-octyloxy-*p*-xylylene) ($X_n \sim 32$) with $\text{Fe}(\text{ClO}_4)_2$; ^1H NMR spectra of **2a** and **2b**; ^{13}C NMR spectrum of **2a**. This material is available free of charge via the Internet at <http://pubs.acs.org>.

References and Notes

- (1) Steiger, D.; Tervoort, T.; Weder, C.; Smith, P. *Macromol. Rapid Commun.* **2000**, *21*, 405.
- (2) (a) Rowan, S. J.; Cantrill, S. J.; Cousins, G. R. L.; Sanders, J. K. M.; Stoddart, J. F. *Angew. Chem., Int. Ed.* **2002**, *41*, 898. (b) Brunsveld, L.; Folmer, B. J. B.; Meijer, E. W.; Sijbesma, R. P. *Chem. Rev.* **2001**, *101*, 4071. (c) Ciferri, A. *Macromol. Rapid Commun.* **2002**, *23*, 511.
- (3) Errede, L. A.; Szwarc, M. *Q. Rev. Chem. Soc.* **1958**, *12*, 301.
- (4) Beach, W. F. *Xylylene Polymers*. In *Encyclopedia of Polymer Science and Technology*, 3rd ed.; Kroschwitz, J., Ed.; John Wiley & Sons: New York, 2004; Vol. 12, p 587 ff.
- (5) Greiner, A.; Mang, S.; Schäfer, O.; Simon, P. *Acta Polym.* **1997**, *48*, 1.
- (6) Szwarc, M. *Polym. Eng. Sci.* **1976**, *16*, 473.
- (7) (a) Errede, L. A.; Knoll, N. J. *Polym. Sci.* **1962**, *60*, 21. (b) Kirkpatrick, D. E.; Wunderlich, B. *Makromol. Chem.* **1985**, *186*, 2595.
- (8) Greiner, A. *Trends Polym. Sci.* **1997**, *5*, 12.
- (9) Gorham, W. F. *J. Polym. Sci., Part A1* **1966**, *4*, 3027.
- (10) (a) Simon, P.; Greiner, A. *Polym. J.* **1992**, *24*, 1317. (b) Simon, P.; Mang, S.; Hasenhiindl, A.; Gronski, W.; Greiner, A. *Macromolecules* **1998**, *31*, 8775.
- (11) Schäfer, O.; Greiner, A. *Macromolecules* **1996**, *29*, 6074.
- (12) Szwarc, M. *Discuss. Faraday Soc.* **1947**, *2*, 46.
- (13) (a) Steiger, D.; Ehrenstein, M.; Weder, C.; Smith, P. *Macromolecules* **1998**, *31*, 1254. (b) Steiger, D.; Weder, C.; Smith, P. *Macromolecules* **1999**, *32*, 5391.
- (14) (a) Schäfer, O.; Greiner, A.; Antonietti, M.; Zisenis, M. *Acta Polym.* **1996**, *47*, 386. (b) Schäfer, O.; Brink-Spalink, F.; Smarsly, B.; Schmidt, C.; Wendorf, J. H.; Witt, C.; Kissel, T.; Greiner, A. *Macromol. Chem. Phys.* **1999**, *200*, 1942. (c) Schäfer, O.; Brink-Spalink, F.; Greiner, A. *Macromol. Rapid Commun.* **1999**, *20*, 190. (d) Brink-Spalink, F.; Greiner, A.; *Macromolecules* **2002**, *35*, 3315. (e) Ishaque, M.; Agarwal, S.; Greiner, A. *e-Polym.* **2002**, Art. No. 31.
- (15) Beck, B. J.; Kokil, A.; Ray, D.; Rowan, S. J.; Weder, C. *Macromolecules* **2002**, *35*, 590.
- (16) (a) Kelch, S.; Rehahn, M. *Macromolecules* **1999**, *32*, 5818. (b) Rehahn, M. *Acta Polym.* **1998**, *49*, 201. (c) Lahn, B.; Rehahn, M. *Macromol. Symp.* **2001**, *163*, 157. (d) Knapp, R.; Schott, A.; Rehahn, M. *Macromolecules* **1996**, *29*, 478. (e) Velten, U.; Rehahn, M. *Chem. Commun.* **1996**, 2639. (f) Schmatloch, S.; van den Berg, A. M. J.; Hofmeier, H.; Schubert, U. S. *Des. Monomers Polym.* **2004**, *7*, 191. (g) Hofmeier, H.; Schmatloch, S.; Wouters, D.; Schubert, U. S. *Macromol. Chem. Phys.* **2003**, *204*, 2197. (h) Schmatloch, S.; van den Berg, A. M. J.; Alexeev, A. S.; Hofmeier, H.; Schubert, U. S. *Macromolecules* **2003**, *36*, 9943. (i) Pollino, J. M.; Nair, K. P.; Stubbs, L. P.; Adams, J.; Weck, M. *Tetrahedron* **2004**, *60*, 7205. (j) Gerhardt, W.; Erne, M.; Weck, M. *Chem.-Eur. J.* **2004**, *10*, 6212.
- (17) El-ghayoury, A.; Schenning, A. P. H. J.; Meijer, E. W. *J. Polym. Sci., Part A: Polym. Chem.* **2002**, *40*, 4020.
- (18) (a) Figgemeier, E.; Merz, L.; Hermann, B. A.; Zimmermann, Y. C.; Housecroft, C. E.; Güntherodt, H.-J.; Constable, E. C. *J. Phys. Chem. B* **2003**, *107*, 1157. (b) Constable, E. C.; Housecroft, C. E.; Neuburger, M.; Schneider, A. G.; Springer, B.; Zehnder, M. *Inorg. Chim. Acta* **2000**, *300–302*, 49. (c) Constable, E. C.; Housecroft, C. E.; Lambert, J. N.; Malarek, D. A. *Chem. Commun.* **2005**, 3739. (d) Hjelm, J.; Hel, R. W.; Hagfeldt, A.; Constable, E. C.; Housecroft, C. E.; Forster, R. J. *Inorg. Chem.* **2005**, *44*, 1073. (e) Hjelm, J.; Handel, R. W.; Hagfeldt, A.; Constable, E. C.; Housecroft, C. E.; Forster, R. J. *Electrochem. Commun.* **2004**, *6*, 193. (f) Hjelm, J.; Constable, E. C.; Figgemeier, E.; Hagfeldt, A.; Handel, R.; Housecroft, C. E.; Mukhtar, E.; Schofield, E. *Chem. Commun.* **2002**, 284. (g) Encinas, S.; Flamigni, L.; Barigelletti, F.; Constable, E. C.; Housecroft, C. E.; Schofield, E.; Figgemeier, E.; Fenske, D.; Neuburger, M.; Vos, J. G.; Zehnder, M. *Chem.-Eur. J.* **2002**, *8*, 137.
- (19) (a) Schütte, M.; Kurth, D. G.; Linford, M. R.; Cölfen, H.; Möhwald, H. *Angew. Chem., Int. Ed.* **1998**, *37*, 2891. (b) Kurth, D. G.; Lehmann, P.; Schütte, M. *Proc. Natl. Acad. Sci. U.S.A.* **2000**, *97*, 5704. (c) Lehmann, P.; Kurth, D. G.; Brezesinski, G.; Symietz, C. *Chem.-Eur. J.* **2001**, *7*, 1646. (d) Kurth, D. G.; Meister, A. F.; Thünemann, A. F.; Förster, G. *Langmuir* **2003**, *19*, 4055. (e) Kurth, D. G.; Severin, N.; Rabe, J. P. *Angew. Chem., Int. Ed.* **2002**, *41*, 3681.
- (20) Dobrawa, R.; Lysetska, M.; Ballester, P.; Grüne, M.; Würthner, F. *Macromolecules* **2005**, *38*, 1315.
- (21) For recent reviews see: (a) Nguyen, P.; Gomes-Elipe, P.; Manners, I. *Chem. Rev.* **1999**, *99*, 1515. (b) Pickup, P. G. *J. Mater. Chem.* **1999**, *9*, 1641. (c) Wolf, M. O. *Adv. Mater.* **2001**, *13*, 545. (d) Schubert, U. S.; Eschbaumer, C. *Angew. Chem., Int. Ed.* **2002**, *41*, 2892. (e) Manners, I. *Synthetic Metal-Containing Polymers*; Wiley-VCH: Weinheim, 2004. (f) Holder, E.; Langeveld, B. M. W.; Schubert, U. S. *Adv. Mater.* **2005**, *17*, 1109. (g) Holliday, B. J.; Swager, T. M. *Chem. Commun.* **2005**, 23.
- (22) For recent examples see: (a) Schmatloch, S.; González, M. F.; Schubert, U. S. *Macromol. Rapid Commun.* **2002**, *23*, 957. (b) Yount, W. C.; Juwarker, H.; Craig, S. L. *J. Am. Chem. Soc.* **2003**, *125*, 15302. (c) Vermonden, T.; van der Gucht, J.; de Waard, P.; Marcelis, A. T. M.; Besseling, N. A. M.; Sudhölter, E. J. R.; Fleer, G. J.; Stuart, M. A. C. *Macromolecules* **2003**, *36*, 7035. (d) Lahn, B.; Rehahn, M. *e-Polym.* **2002**, *1*, 1. (e) Loveless, D. M.; Jeon, S. L.; Craig, S. L. *Macromolecules* **2005**, *38*, 10171. (f) Yount, W. C.; Loveless, D. M.; Craig, S. L. *J. Am. Chem. Soc.* **2005**, *127*, 14488. (g) Schmittel, M.; Kalsani, V.; Kishore, R. S. K.; Cölfen, H.; Bats, J. W. *J. Am. Chem. Soc.* **2005**, *127*, 11544.
- (23) (a) Iyer, P. K.; Beck, J. B.; Weder, C.; Rowan, S. J. *Chem. Commun.* **2005**, 319. (b) Knapton, D.; Rowan, S. J.; Weder, C. *Macromolecules* **2006**, *39*, 651.
- (24) (a) Petoud, S.; Bünzli, J.-C. G.; Schenk, K. J.; Piguet, C. *Inorg. Chem.* **1997**, *36*, 1345. (b) Nozary, H.; Piguet, C.; Tissot, P.; Bernardinelli, G.; Bünzli, J.-C. G.; Deschenaux, R.; Guillon, D. *J. Am. Chem. Soc.* **1998**, *120*, 12274. (c) Nozary, H.; Piguet, C.; Rivera, J.-P.; Tissot, P.; Bernardinelli, G.; Vulliermet, N.; Weber, J.; Bünzli, J.-C. G. *Inorg. Chem.* **2000**, *39*, 5286. (d) Nozary, H.; Piguet, C.; Rivera, J.-P.; Tissot, P.; Morgantini, P.-Y.; Weber, J.; Bernardinelli, G.; Bünzli, J.-C. G.; Deschenaux, R.; Donnio, B.; Guillon, D. *Chem. Mater.* **2002**, *14*, 1075. (e) Terazzi, E.; Torelli, S.; Bernardinelli, G.; Rivera, J.-P.; Benech, J.-M.; Bourgogne, C.; Donnio, B.; Guillon, D.; Imbert, D.; Bünzli, J.-C. G.; Pinto, A.; Jeannerat, D.; Piguet, C. *J. Am. Chem. Soc.* **2005**, *127*, 889.
- (25) (a) Beck, J. B.; Rowan, S. J. *J. Am. Chem. Soc.* **2003**, *125*, 13922. (b) Zhao, Y.; Beck, J. B.; Rowan, S. J.; Jamieson, A. M. *Macromolecules* **2004**, *37*, 3529. (c) Rowan, S. J.; Beck, J. B. *Faraday Discuss.* **2005**, *128*, 43. (d) Beck, J. B.; Ineman, J. M.; Rowan, S. J. *Macromolecules* **2005**, *38*, 5060.
- (26) (a) Hahn, S. F. *J. Polym. Sci., Part A: Polym. Chem.* **1992**, *30*, 397. (b) Hillmyer, M. A.; Laredo, W. R.; Grubbs, R. H. *Macromolecules* **1995**, *28*, 6311. (c) Wagener, K. B.; Valenti, D.; Hahn, S. F. *Macromolecules* **1997**, *30*, 6688.
- (27) (a) Mori, T.; Takamoto, M.; Wada, T.; Inoue, Y. *Helv. Chim. Acta* **2001**, *84*, 2693. (b) Lindeman, S. V.; Rosokha, S. V.; Sun, D.; Kochi, J. K. *J. Am. Chem. Soc.* **2002**, *124*, 843.
- (28) (a) Weder, C.; Wrighton, M. S. *Macromolecules* **1996**, *29*, 5157. (b) Voskerician, G.; Weder, C. *Adv. Polym. Sci.* **2005**, *177*, 209.
- (29) (a) Krumholz, P. *Inorg. Chem.* **1965**, *4*, 612. (b) El-ghayoury, A.; Schenning, A. P. H. J.; Meijer, E. W. *J. Polym. Sci., Part A: Polym. Chem.* **2002**, *40*, 4020.
- (30) Piguet, C.; Williams, A. F.; Bernardinelli, G.; Bünzli, J.-C. G. *Inorg. Chem.* **1993**, *32*, 4139.
- (31) Huang, W. Y.; Gao, W.; Kwei, T. K.; Okamoto, Y. *Macromolecules* **2001**, *34*, 1570.

MA060500Y